Translational Oncology
www.transonc.com

Volume 6 Number 4 August 2013 pp. 413–419 413

Dasatinib Inhibits DNA Repair after Radiotherapy Specifically in pSFK-Expressing Tumor Areas in Head and Neck Xenograft Tumors[1]

Hanneke Stegeman*, Paul N. Span*, Paul F. J. W. Rijken*, Simone C. Cockx*, Deric L. Wheeler†, Mari Iida†, Albert J. van der Kogel*,†, Johannes H. A. M. Kaanders* and Johan Bussink*

*Department of Radiation Oncology, Radboud University Nijmegen Medical Centre, Nijmegen, The Netherlands; †Department of Human Oncology, University of Wisconsin School of Medicine and Public Health, Madison, WI

Abstract

Src family kinases (SFKs) have been implicated in resistance to both radiation and epidermal growth factor receptor (EGFR) inhibition. Therefore, we investigated whether inhibition of SFK through dasatinib (DSB) can enhance the effect of radiotherapy in two *in vivo* human head and neck squamous cell carcinoma (HNSCC) models. Response to DSB and/or radiotherapy was assessed with tumor growth delay assays in two HNSCC xenograft models, SCCNij153 and SCCNij202. Effects on EGFR signaling were evaluated with Western blot analysis, and effects on DNA repair, hypoxia, and proliferation were investigated with immunohistochemistry. DSB and radiotherapy induced a significant growth delay in both HNSCC xenograft models, although to a lesser extent in SCCNij202. DSB did not inhibit phosphorylated protein kinase B (pAKT) or phosphorylated extracellular signal–regulated kinase 1/2 (pERK1/2) but did inhibit (phosphorylated) DNA-dependent protein kinase. Moreover, DSB reduced repair of radiation-induced DNA double-strand breaks as shown by an increase of p53-binding protein 1 (53BP1) staining 24 hours after radiation. This effect on DNA repair was only observed in the cell compartment where phosphorylated SFK (pSFK) was expressed: for SCCNij153 tumors in both normoxic and hypoxic areas and for SCCNij202 tumors only in hypoxic areas. No consistent effects of DSB on hypoxia or proliferation were observed. In conclusion, DSB enhances the effect of radiotherapy *in vivo* by inhibition of radiation-induced DNA repair and is a promising way to improve outcome in HNSCC patients.

Translational Oncology (2013) 6, 413–419

Introduction

Overexpression of the epidermal growth factor receptor (EGFR) is a frequent event in head and neck squamous cell carcinoma (HNSCC) and is associated with a worse prognosis after radiotherapy [1]. Accordingly, a randomized clinical trial has shown that addition of cetuximab, a chimeric monoclonal antibody against the extracellular part of EGFR, improves the clinical outcome in HNSCC patients treated with radiotherapy [2]. However, locoregional control at 3 years was only improved from 34% in the group treated with radiotherapy alone to 47% in the group treated with radiotherapy and cetuximab combined, while most patients experienced additional side effects due to the addition of cetuximab [2]. Hence, to further improve outcome in these patients, it will be essential to develop therapeutic strategies that target other molecules of the EGFR signaling network involved in resistance to radiotherapy.

Src family kinases (SFKs) are non-receptor kinases involved in pathways that control cell division, motility, adhesion, angiogenesis, and survival [3,4]. It has been shown that SFKs interact with growth factor signaling, including signaling through EGFR [5–7]. More importantly,

Address all correspondence to: Hanneke Stegeman, MSc, Department of Radiation Oncology, Radboud University Nijmegen Medical Centre, PO Box 9101, 6500 HB Nijmegen, The Netherlands. E-mail: h.stegeman@rther.umcn.nl

[1]This project was financially supported by the Dutch Cancer Society (grant 2008-4000) and in part by the Clinical and Translational Science Award program through the National Institutes of Health (NIH) National Center for Advancing Translational Sciences (grant UL1TR000427 to D.L.W.). The content is solely the responsibility of the authors and does not necessarily represent the official views of the NIH. No conflicts of interests are present.
Received 7 March 2013; Revised 8 April 2013; Accepted 12 April 2013

 1944-7124/13/$25.00
DOI 10.1593/tlo.13259

activated SFKs are required for the nuclear translocation of EGFR induced by cetuximab or radiation [8,9]. Nuclear EGFR increases DNA repair through interaction with DNA-dependent protein kinase (DNA-PK) and consequently decreases radiosensitivity [10]. Although radiation-induced translocation of EGFR to the nucleus can be blocked by cetuximab [11], nuclear EGFR is also a cause of resistance to cetuximab [12]. Therefore, inhibition of nuclear EGFR through inhibition of SFKs could enhance radiosensitivity by decreasing repair of radiation-induced DNA damage.

Activity of SFKs can be inhibited by dasatinib (DSB), a small molecule tyrosine kinase inhibitor that also inhibits other kinases, including ABL [13]. DSB inhibits the *in vitro* growth of different tumor lines [13], including head and neck cancer lines [14]. However, SFK inhibition does not seem to have large effects on tumor growth *in vivo* [15,16] and also the clinical efficacy of DSB as a single agent in HNSCC seems low despite effective c-Src inhibition [17]. Nevertheless, the important role of SFKs in growth factor signaling and nuclear translocation of EGFR makes DSB an interesting candidate for enhancing the efficacy of radiotherapy in HNSCC. A recent study by Raju et al. [18] has indeed shown that DSB enhances radiosensitivity in HNSCC cells *in vitro* through inhibition of nuclear EGFR and by decreasing radiation-induced DNA repair. However, the tumor microenvironment, which exposes tumor cells to fluctuating oxygen and nutrient gradients, can have a great impact on tumor behavior and tumor response. Therefore, it is of great importance to determine the effects of DSB and radiotherapy in the context of the tumor microenvironment in *in vivo* models before these results can be translated to the clinic.

In this study, we investigated the potential of combining DSB with radiotherapy *in vivo* by analyzing the effects of DSB and radiotherapy on tumor growth, EGFR signaling, and DNA repair in two human HNSCC xenograft models. These HNSCC models both show high EGFR expression [19] but differ in their expression level of phosphorylated SFK (pSFK). In addition, the effects on hypoxia and proliferation, two important mechanisms involved in resistance to radiotherapy, were examined.

Materials and Methods

Xenograft Tumor Models and Treatment

Tumor models SCCNij153 and SCCNij202 were derived from human larynx carcinomas. Viable 1-mm^3 tumor pieces were implanted subcutaneously in 6- to 10-week-old athymic BALB/c nu/nu mice and passaged at a diameter of 1 cm. Tumors with a mean diameter of 4 to 5 mm transplanted at the hind leg were used in the experiments.

Animals were treated with DSB (70 mg/kg per day, oral; LC Laboratories, Woburn, MA) for 5 days, 10 Gy single-dose radiotherapy (320 kV, dose rate of 3.8 Gy/min, X-RAD; RPS Services Limited, Surrey, United Kingdom), or a combination of DSB and 10 Gy radiotherapy (given on day 4 of DSB treatment).

For effects on tumor growth delay, tumor diameters were measured twice a week in three perpendicular directions and tumor volumes were determined by the following formula: $V = (a * b * c * \pi)/6$. Endpoint was reached when the tumor volume tripled compared to the volume at start of treatment. Maximal follow-up was 60 days.

For effects on protein expression, proliferation, and hypoxia, tumors were harvested 1 day after 10 Gy radiotherapy and/or on day 5 of DSB treatment. One hour before euthanasia, animals were injected with 80 mg/kg of the hypoxia marker pimonidazole hydrochloride (1-[(2-hydroxy-3-piperidinyl)propyl]-2-nitroimidazole hydrochloride; Natural Pharmaceuticals International Inc, Research Triangle Park, NC) and 15 minutes before euthanasia with 50 mg/kg of the proliferation marker bromodeoxyuridine (BrdU; Sigma, St Louis, MO). After excision, tumors were snap frozen in liquid nitrogen.

Animals were kept in a specific pathogen-free unit in accordance with institutional guidelines. All experiments were approved by the Animal Experiments Committee of the Radboud University Nijmegen Medical Centre.

Western Blot Analysis

Tumor sections were lysed in NP-40 lysis buffer and protein was quantitated using a standard Bradford absorbance assay. Proteins (35 μg per lane) were separated by sodium dodecyl sulfate–polyacrylamide gel electrophoresis and blotted onto polyvinylidene fluoride (PVDF) membrane. Membranes were incubated with the appropriate primary antibodies followed by incubation with HRP-conjugated antibodies and proteins were detected with an ECL chemiluminescence system. Antibodies against the following antigens were used: EGFR, protein kinase B (AKT), and HRP-conjugated goat anti-mouse IgG were purchased from Santa Cruz Biotechnology (Santa Cruz, CA). DNA-PK, phosphorylated DNA-PK (pDNA-PK, S2056), SFK, (pSFK, Y416), phosphorylated protein kinase B (pAKT; S473), extracellular signal–regulated kinase 1/2 (ERK1/2), phosphorylated extracellular signal–regulated kinase 1/2 (pERK1/2; T202/Y204), and HRP-conjugated goat anti-rabbit IgG were purchased from Cell Signaling Technology (Beverly, MA), and α-tubulin was obtained from Calbiochem (San Diego, CA).

Immunohistochemical Staining

For quantification of hypoxia and proliferation, frozen tumor sections (5 μm) were stained for pimonidazole and BrdU, respectively, vessels and nuclei. For quantification of DNA damage, tumor sections were stained for p53-binding protein 1 (53BP1) or Rad51, pimonidazole, vessels, and nuclei. To evaluate colocalization of pSFK and hypoxia, tumor sections were stained for pSFK (Y416), pimonidazole, and vessels.

The antibody against pimonidazole was a gift from J. A. Raleigh (University of North Carolina). Vessels were detected with 9F1, a rat monoclonal antibody against mouse endothelium (Department of Pathology, Radboud University Nijmegen Medical Centre). The antibody against BrdU was purchased from Genetex (Irvine, CA), antibody against 53BP1 from Thermo Scientific (Waltham, MA), and the antibody against Rad51 from Epitomics (Burlingame, CA).

Primary antibodies were detected by appropriate Cy3-conjugated (Jackson ImmunoResearch Laboratories Inc, West Grove, PA), Alexa 488–, Alexa 647–, or Alexa 55–conjugated (Molecular Probes, Leiden, The Netherlands) secondary antibodies. All secondary antibodies were tested for specificity for the primary antibody by performing the staining procedures without the primary antibody. Nuclei were stained with Hoechst 33342 (Sigma) or 4′,6-diamidino-2-phenylindole (DAPI; Abcam, Cambridge, United Kingdom).

Image Acquisition and Computerized Analysis of DNA Repair

Approximately eight single fields were randomly chosen and recorded in tumor sections stained for 53BP1 or Rad51 using a fluorescence microscope (Zeiss, Göttingen, Germany). Each single field

was acquired with different filters at ×400 magnification to yield images of the different fluorescent signals. Single fields were acquired in both normoxic and hypoxic tumor areas based on pimonidazole staining. Gray value images of 53BP1, Rad51, and nuclei were converted to binary images by setting thresholds for the fluorescence signals above the background using ImageJ software (NIH, Bethesda, MD). Hypoxic tumor areas were delineated using the pimonidazole gray value images. The nuclear area positive for 53BP1 or Rad51 and the number of nuclei were quantified in hypoxic and normoxic regions separately. The average area positive for 53BP1 or Rad51 per nucleus was calculated by dividing the total nuclear area of 53BP1 or Rad51 by the total number of nuclei. At least 600 nuclei per tumor section were analyzed.

Image Acquisition and Computerized Analysis of Hypoxia and Proliferation

Stained tumor sections were scanned with a fluorescence microscope (Zeiss). Each section was sequentially scanned at ×100 magnification to yield images of the different fluorescent signals. Thresholds for the fluorescence signals were interactively set above the background and the gray value images were converted to binary images. The hypoxic fraction (HF) was calculated by dividing the tumor area positive for pimonidazole by the total tumor area and the BrdU labeling index (LI) by dividing the nuclear area positive for BrdU by the total nuclear area of the tumor, as described before [20,21]. Necrotic areas and staining artifacts were excluded from analysis.

Statistics

Tumor growth delay data were analyzed using Kaplan-Meier survival curves and Cox proportional-hazards regression. To determine whether DSB and radiotherapy had a synergistic effect on growth delay, the relative excess risk due to interaction (RERI) was calculated as described by Andersson et al. [22]. RERI values above 0 indicate biologic interaction between treatments.

Changes in hypoxia, proliferation, and DNA damage after treatment were tested for significance using unpaired *t* tests. All tests were performed using Prism (GraphPad Software, Inc, La Jolla, CA), and P values < .05 were considered significant.

Results

Combining DSB with Radiotherapy Induces Significantly Enhanced Growth Delay in HNSCC Xenograft Tumors

SCCNij153 and SCCNij202 tumors both expressed high levels of EGFR and phosphorylated EGFR (pEGFR), indicating active EGFR signaling in these tumor models (Figure 1*A*). SFKs and their activated forms were also expressed in both tumor models, although the level of pSFK was markedly lower in SCCNij202 tumors (Figure 1*A*).

In both SCCNij153 and SCCNij202, the combination of DSB and radiotherapy significantly delayed tumor growth compared to untreated tumors (P < .05), while DSB or radiotherapy alone did not induce a significant delay (Figure 1*B*). These results indicate a synergistic effect of DSB and radiotherapy, and RERI values of 2.0 and 0.70 for SCCNij153 and SCCNij202, respectively, confirm this interaction. Although significant, the absolute delay in growth was small in SCCNij202 tumors, as is also reflected by the relative low RERI value of 0.70.

DSB Inhibits DNA-PK but Not AKT or ERK Signaling

Using Western blot analyses, clear inhibition of pSFK was observed in both tumor models when tumors were treated with DSB or the combination of DSB and radiotherapy (Figure 2). DSB also decreased EGFR in SCCNij202 tumors but not in SCCNij153 tumors, while DSB slightly decreased pAKT in SCCNij153 tumors. However, no large effects on pAKT or pERK1/2 levels were observed in both tumor models after radiotherapy, DSB, or combined treatment. In

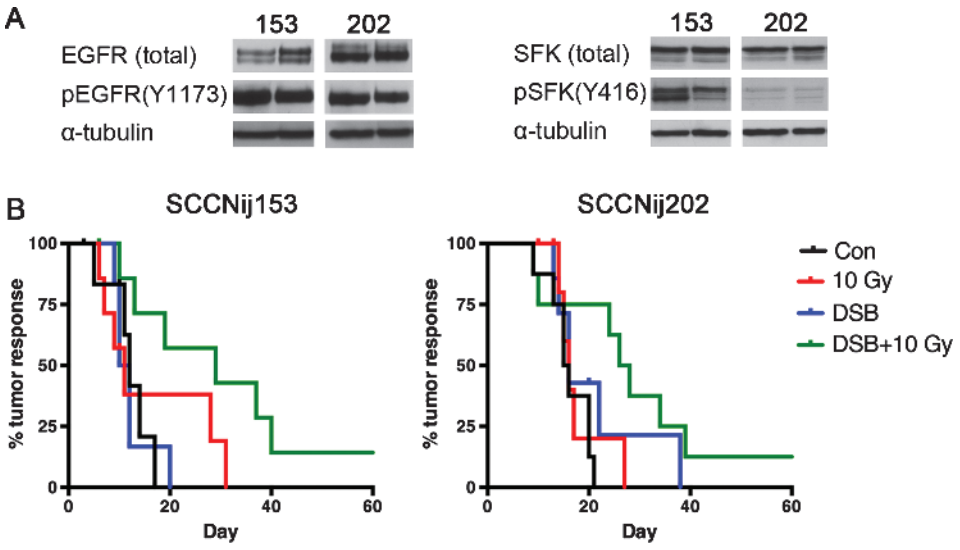

Figure 1. Expression of EGFR and pSFK and effects of DSB and/or radiotherapy on tumor growth delay. (A) Expression of (p)EGFR and (p)SFK in untreated SCCNij153 and SCCNij202 tumors. Two tumors per line were analyzed and both tumor lines were blotted on the same membrane. α-Tubulin was used as loading control. (B) Kaplan-Meier survival curves showing the effect of DSB and/or radiotherapy on the tumor growth of SCCNij153 and SCCNij202. Events were scored when the tumor volume tripled compared to the start volume and % tumor response represents the percentage of tumors that did not reach the event. Tumors were treated with DSB (five times 70 mg/kg), 10 Gy radiotherapy, or combined DSB and radiotherapy. Number of animals per group: six to eight.

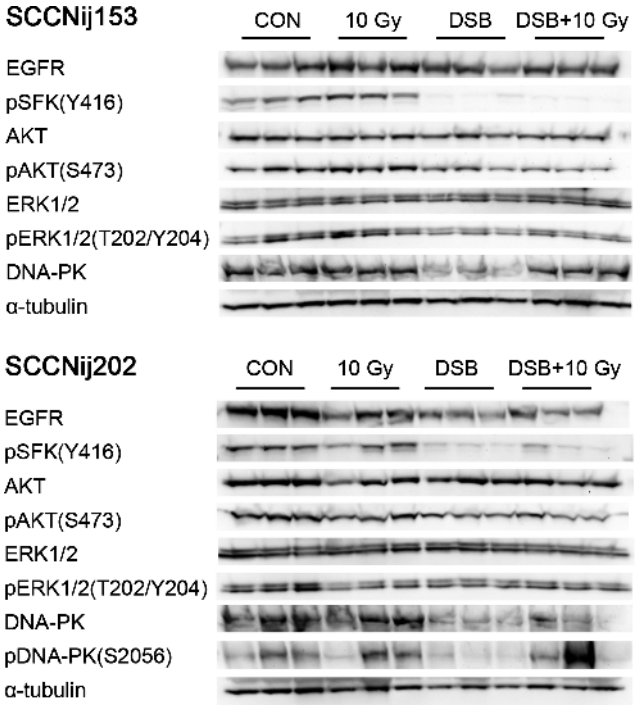

Figure 2. Effects of DSB and/or radiotherapy on EGFR signaling. Expression of EGFR, pSFK, (p)AKT, (p)ERK1/2, and (p)DNA-PK in SCCNij202 and SCCNij153 tumors. α-Tubulin was used as loading control. Tumors were treated with DSB (five times 70 mg/kg), 10 Gy radiotherapy, or combined DSB and radiotherapy. Tumors were harvested 24 hours after radiotherapy or after the fifth DSB treatment. Three tumors per line were analyzed and tumor lines were blotted on separate membranes.

contrast, DNA-PK levels were clearly decreased by DSB in both tumor models. Activated DNA-PK (pDNA-PK) was also inhibited by DSB in SCCNij202 tumors, although variation was present in tumors treated with combined DSB-radiotherapy treatment. In SCCNij153 tumors, pDNA-PK levels were non-detectable and effects of treatment could not be assessed.

DSB Increases Residual DNA Damage after Radiotherapy but Only in the Tumor Compartment Where pSFK Is Expressed

To determine whether decreased DNA-PK levels resulted in reduced repair of DNA double strand breaks, tumors were harvested 24 hours after radiotherapy with and without DSB and immunofluorescently stained for 53BP1. In SCCNij153 tumors, the area of 53BP1 per nucleus increased when DSB was combined with radiotherapy compared to radiotherapy alone in both hypoxic and normoxic tumor regions ($P < .01$; Figure 3*A*). This indicates increased residual DNA damage and thus a reduction of DNA repair due to DSB. In SCCNij202 tumors, only hypoxic regions showed increased 53BP1 staining after addition of DSB ($P < .01$).

Rad51 staining was also analyzed to determine the effects on DNA repair by homologous recombination (HR; Figure 3*B*). Again, the Rad51 area was increased in both hypoxic (n.s.) and normoxic ($P < .05$) regions of SCCNij153 tumors treated with DSB and radiotherapy compared to radiotherapy alone, while in SCCNij202 this effect of DSB was only observed in hypoxic regions ($P < .01$).

The hypoxia-specific effects of DSB in SCCNij202 tumors could be due to a higher expression of pSFK under influence of hypoxia in this tumor model. Therefore, untreated tumors of both SCCNij153 and SCCNij202 were immunofluorescently stained for pSFK and hypoxia (Figure 4). In SCCNij153, pSFK was widely expressed in both

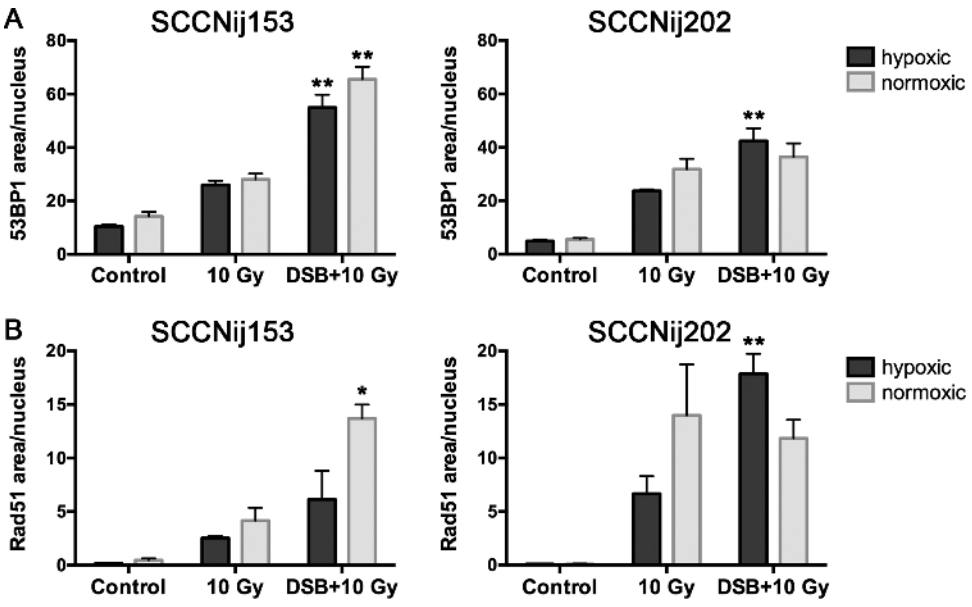

Figure 3. Effects of DSB and/or radiotherapy on residual DNA damage. Average area positive for 53BP1 (A) or Rad51 (B) per nucleus in untreated tumors and tumors harvested 24 hours after treatment with radiotherapy (10 Gy) or DSB (five times 70 mg/kg) and radiotherapy. Differences between 10 Gy and DSB + 10 Gy in hypoxic or normoxic areas were tested for significance using *t* tests, $*P < .05$, $**P < .01$. Error bars represent SEM. Number of animals per group: three to four.

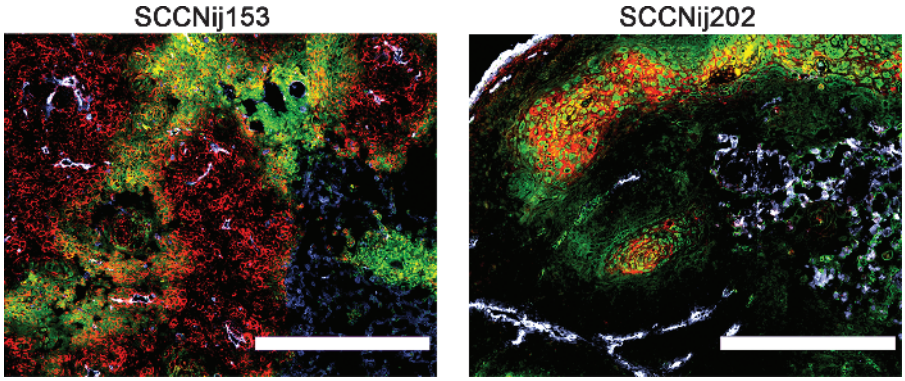

Figure 4. Expression of pSFK in relation to hypoxia in SCCNij153 and SCCNij202. Expression of pSFK in relation to hypoxia was visualized by immunofluorescence staining in untreated SCCNij153 and SCCNij202 tumors. pSFK, red; hypoxia, green; vessels, blue. Non-specific staining present in necrotic regions. Scale bars represent 500 μm. Original magnification, ×200.

normoxic and hypoxic regions of the tumor, while pSFK expression in SCCNij202 tumors was restricted to hypoxic regions of the tumor. This difference in pSFK expression pattern between SCCNij153 and SCCNij202 is also reflected in total pSFK levels of these tumors as observed with Western blot (Figure 1*A*).

Hence, these data indicate that DSB reduces radiation-induced DNA repair and that this effect is restricted to regions of the tumor where pSFK is expressed.

No Effect of DSB on Hypoxia or Proliferation

No consistent effects of DSB on hypoxia or proliferation were observed (Figure 5). Only the combination of DSB and radiotherapy reduced proliferation significantly in SCCNij202 ($P < .05$), while DSB alone did not induce any reduction in proliferation.

Discussion

In the present study, we show that DSB enhances the effect of radiotherapy in two HNSCC xenograft models with EGFR expression. Moreover, we show that this interaction is likely due to inhibition of pSFK-mediated activation of DNA-PK by DSB, resulting in increased residual DNA damage after radiotherapy. However, the effects on tumor growth delay and DNA repair differed between tumor models, which has important implications for further research.

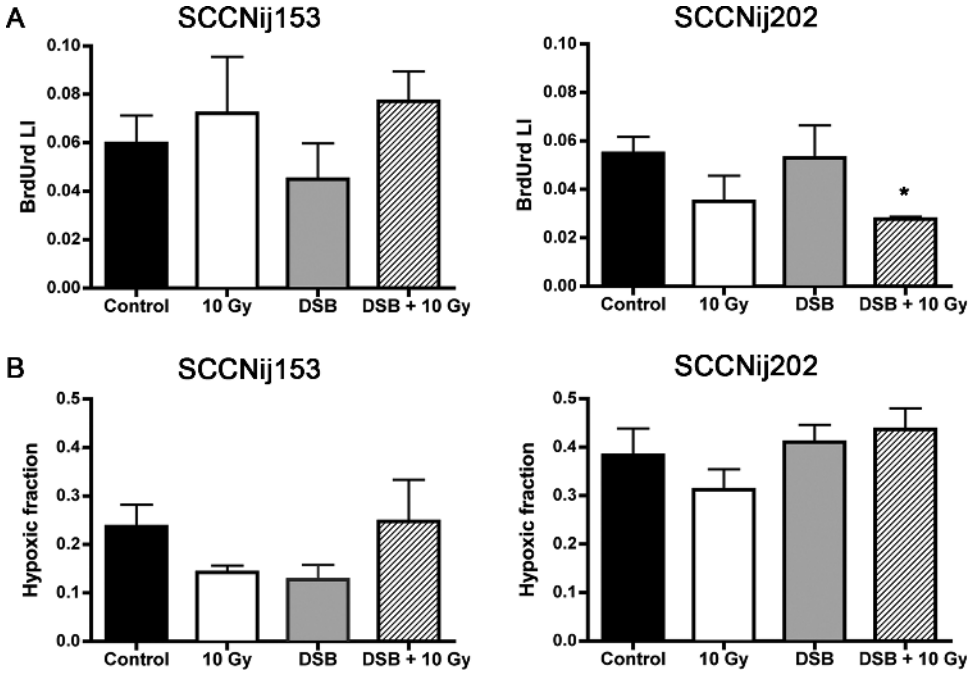

Figure 5. Effects of DSB and/or radiotherapy on proliferation and hypoxia. Effects of DSB and/or radiotherapy on the BrdU LI (A) and hypoxic fraction (HF; B). Tumors were treated with DSB (five times 70 mg/kg), 10 Gy radiotherapy, or combined DSB and radiotherapy. Tumors were harvested 24 hours after radiotherapy or after the fifth DSB treatment. Differences between treatment groups were tested for significance using *t* tests, $*P < .05$. Error bars represent SEM. Number of animals per group: three to four.

DSB has earlier been shown to induce degradation of EGFR and consequently inhibition of downstream pAKT and pERK1/2, resulting in induction of apoptosis in HNSCC *in vitro* [23]. In addition, Raju et al. reported that DSB only enhances radiation sensitivity in HNSCC cell lines in which DSB reduces pAKT levels [18]. Moreover, activation of AKT by radiation has been observed in various *in vitro* models, while Kim et al. established that c-Src signaling is involved in this activation of AKT [24]. Although EGFR levels were slightly reduced after DSB treatment in SCCNij202, we neither observed activation of pAKT or pERK1/2 after radiation nor inhibition of pAKT or pERK1/2 after DSB treatment. This lack of change in pAKT and pERK1/2 levels could be due to activating factors present in our *in vivo* tumor models that are not present in the *in vitro* cell culture conditions applied by others [18,23,24]. In the study of Lin et al., cells can be rescued from DSB-induced apoptosis by increasing EGFR activation through ligand administration [23]. We did not measure EGFR ligand levels, but as both tumor models show high phosphorylated EGFR levels, it is likely that these ligands are indeed present in our tumor models. In addition, we have shown that *in vivo* expression of these kinases can be substantially affected by the tumor microenvironment [25]. The lack of inhibition of pERK1/2 and pAKT by DSB is also consistent with the observation that DSB alone did not have an effect on growth delay in either of our tumor models.

In contrast to pAKT and pERK1/2, we did observe significant inhibition of DNA-PK by DSB. In addition, pDNA-PK levels were decreased in SCCNij202 tumors treated with DSB. In SCCNij153 tumors, pDNA-PK levels were below the detection limits and we could not confirm inhibition by DSB in this tumor model. Western blot analysis of whole tumor lysates also includes non-tumor tissue and this could decrease the expression levels of tumor proteins. This can make detection of proteins expressed at very low levels, like pDNA-PK, very difficult. EGFR signaling has been shown to affect DNA-PK activity by two ways, i.e., by indirect activation through the phosphatidylinositol 3-kinase (PI3-K)-AKT pathway (cytoplasmic pathway) or by direct interaction between EGFR and DNA-PK after translocation of EGFR to the nucleus (nuclear pathway) [26]. pSFK is involved in the nuclear translocation of EGFR and our observations that DNA-PK is inhibited by DSB independent of pAKT levels suggests that DSB blocks only the nuclear signaling pathway of EGFR in our tumor models but not the cytoplasmic pathways.

Importantly, we further observed that irradiated tumors that also received DSB showed an increase in residual DNA damage as detected by 53BP1 staining, which indicates that the inhibition of DNA-PK resulted in a functional reduction of DNA repair. Hence, our data indicate that DSB enhances radiosensitivity *in vivo* by inhibition of radiation-induced DNA repair. DNA double strand breaks can be repaired through two main pathways: non-homologous end joining and HR [27]. DNA-PK is a key protein of non-homologous end joining, which acts throughout the cell cycle and repairs the majority of all DNA double strand breaks. However, we also observed an effect of DSB on radiation-reduced repair through HR as we detected increased levels of Rad51, a key protein in HR. Inhibition of EGFR signaling has been shown to regulate HR, but this seems to be regulated through the cytoplasmic and not the nuclear pathway of EGFR [28].

HR acts only in S and G_2 phases of the cell cycle. The observed effect of DSB on HR cannot, however, be explained by changes in cell cycle distribution. No effects on proliferation by DSB were observed in SCCNij153, and although combined DSB-radiotherapy did decrease proliferation in SCCNij202 compared to untreated tumors, a decrease in proliferation should result in a decrease in Rad51 and not an increase as we observed. Several other mechanisms could explain the effect of DSB on HR. It has been shown that inhibition of DNA-PK activity increases the activity of HR, suggesting that the observed increase in Rad51 is due to a compensatory increase of double strand breaks repaired through HR [29]. Lastly, DSB targets many kinases and the effect on HR could be independent of pSFK inhibition. Nonetheless, the observation that the effect of DSB on DNA repair was only present in the tissue compartment where pSFK is expressed does suggest that pSFK is involved in the effect on DNA repair.

We observed striking differences in the expression pattern of pSFK between the two tumor models. pSFK was expressed diffusely throughout the tumors in SCCNij153 and only expressed in hypoxic regions in SCCNij202. This differential expression pattern probably explains the smaller effect of DSB on growth delay in SCCNij202 as only the hypoxic cells could be targeted by DSB in this tumor model. Both *in vitro* and *in vivo* studies have shown that pSFK is involved in the hypoxic response of tumor cells and is important for cell survival under hypoxic conditions [30,31]. The hypoxia-dependent expression of pSFK in SCCNij202 thus seems a more "physiological" response, while the diffuse expression in SCCNij153 indicates constitutive activation of SFKs, which can arise through multiple mechanisms [3]. Hence, the expression pattern of pSFK could be an important predictive biomarker for response to combined treatment with DSB and radiotherapy.

Next to lower pSFK expression, the modest growth delay in SCCNij202 is also due to large variation in growth delay that was induced by DSB and radiotherapy in this tumor model; some tumors reached the endpoint at time points comparable to controls, while other tumors showed a clear growth delay. In addition, the variation in pDNA-PK levels between tumors treated with DSB and radiotherapy demonstrates the variation in response to treatment. This variation is probably also due to the hypoxia-related expression pattern of pSFK in this tumor model. This expression pattern suggests that tumors with a higher HF will have a higher pSFK fraction. Although we treated all tumors at approximately the same volume, the extent of hypoxia varied between these tumors. Using immunofluorescence, we did indeed observe that untreated tumors with a higher HF also had a higher pSFK fraction (data not shown), although the number of tumors is too low to draw firm conclusions. Together, these data suggest that tumors with a higher HF have a higher fraction of cells that can be targeted by DSB, resulting in a larger effect on tumor growth. Thus, even tumors of the same tumor model can differ significantly in their response due to small differences in tumor microenvironmental parameters. DSB itself did not affect microenvironmental characteristics that are relevant for radiosensitivity, i.e., hypoxia and proliferation. The combination of DSB and radiotherapy only reduced proliferation in SCCNij202 tumors. However, as we measured tumor cell proliferation only at 24 hours after radiotherapy, we possibly missed the effect of DSB and radiotherapy on proliferation in SCCNij153 tumors. At 24 hours after radiotherapy, there can be BrdU labeling of cells that are doomed to die after one or two cell divisions and effects due to these doomed cells cannot be excluded.

In conclusion, DSB has the potential to enhance the efficacy of radiotherapy *in vivo* by inhibition of radiation-induced DNA repair. DSB is thus a promising additive to radiotherapy to improve outcome in patients. However, the extent of effects differed between tumor models and further investigation is warranted to determine which tumor characteristics are predictive for response (e.g., EGFR and pSFK

expression levels, HF). Addition of another kinase inhibitor, like a pAKT inhibitor, which blocks cytoplasmic pathways important for radiation resistance could enhance outcome even further. This knowledge will be critical for optimal use of the combination of DSB and radiotherapy in the clinic.

Acknowledgments

We thank J. Lok and H. Peters for their excellent technical assistance.

References

[1] Ang KK, Berkey BA, Tu X, Zhang HZ, Katz R, Hammond EH, Fu KK, and Milas L (2002). Impact of epidermal growth factor receptor expression on survival and pattern of relapse in patients with advanced head and neck carcinoma. *Cancer Res* **62**, 7350–7356.

[2] Bonner JA, Harari PM, Giralt J, Azarnia N, Shin DM, Cohen RB, Jones CU, Sur R, Raben D, Jassem J, et al. (2006). Radiotherapy plus cetuximab for squamous-cell carcinoma of the head and neck. *N Engl J Med* **354**, 567–578.

[3] Summy JM and Gallick GE (2003). Src family kinases in tumor progression and metastasis. *Cancer Metastasis Rev* **22**, 337–358.

[4] Yeatman TJ (2004). A renaissance for SRC. *Nat Rev Cancer* **4**, 470–480.

[5] Biscardi JS, Maa MC, Tice DA, Cox ME, Leu TH, and Parsons SJ (1999). c-Src-mediated phosphorylation of the epidermal growth factor receptor on Tyr^{845} and Tyr^{1101} is associated with modulation of receptor function. *J Biol Chem* **274**, 8335–8343.

[6] Koppikar P, Choi SH, Egloff AM, Cai Q, Suzuki S, Freilino M, Nozawa H, Thomas SM, Gooding WE, Siegfried JM, et al. (2008). Combined inhibition of c-Src and epidermal growth factor receptor abrogates growth and invasion of head and neck squamous cell carcinoma. *Clin Cancer Res* **14**, 4284–4291.

[7] Zhang Q, Thomas SM, Xi S, Smithgall TE, Siegfried JM, Kamens J, Gooding WE, and Grandis JR (2004). SRC family kinases mediate epidermal growth factor receptor ligand cleavage, proliferation, and invasion of head and neck cancer cells. *Cancer Res* **64**, 6166–6173.

[8] Wheeler DL, Iida M, Kruser TJ, Nechrebecki MM, Dunn EF, Armstrong EA, Huang S, and Harari PM (2009). Epidermal growth factor receptor cooperates with Src family kinases in acquired resistance to cetuximab. *Cancer Biol Ther* **8**, 696–703.

[9] Li C, Iida M, Dunn EF, and Wheeler DL (2010). Dasatinib blocks cetuximab- and radiation-induced nuclear translocation of the epidermal growth factor receptor in head and neck squamous cell carcinoma. *Radiother Oncol* **97**, 330–337.

[10] Dittmann K, Mayer C, Fehrenbacher B, Schaller M, Raju U, Milas L, Chen DJ, Kehlbach R, and Rodemann HP (2005). Radiation-induced epidermal growth factor receptor nuclear import is linked to activation of DNA-dependent protein kinase. *J Biol Chem* **280**, 31182–31189.

[11] Dittmann K, Mayer C, and Rodemann HP (2005). Inhibition of radiation-induced EGFR nuclear import by C225 (Cetuximab) suppresses DNA-PK activity. *Radiother Oncol* **76**, 157–161.

[12] Li C, Iida M, Dunn EF, Ghia AJ, and Wheeler DL (2009). Nuclear EGFR contributes to acquired resistance to cetuximab. *Oncogene* **28**, 3801–3813.

[13] Montero JC, Seoane S, Ocana A, and Pandiella A (2011). Inhibition of SRC family kinases and receptor tyrosine kinases by dasatinib: possible combinations in solid tumors. *Clin Cancer Res* **17**, 5546–5552.

[14] Johnson FM, Saigal B, Talpaz M, and Donato NJ (2005). Dasatinib (BMS-354825) tyrosine kinase inhibitor suppresses invasion and induces cell cycle arrest and apoptosis of head and neck squamous cell carcinoma and non–small cell lung cancer cells. *Clin Cancer Res* **11**, 6924–6932.

[15] Ammer AG, Kelley LC, Hayes KE, Evans JV, Lopez-Skinner LA, Martin KH, Frederick B, Rothschild BL, Raben D, Elvin P, et al. (2009). Saracatinib impairs head and neck squamous cell carcinoma invasion by disrupting invadopodia function. *J Cancer Sci Ther* **1**, 52–61.

[16] Sen B, Peng S, Woods DM, Wistuba I, Bell D, El-Naggar AK, Lai SY, and Johnson FM (2012). STAT5A-mediated SOCS2 expression regulates Jak2 and STAT3 activity following c-Src inhibition in head and neck squamous carcinoma. *Clin Cancer Res* **18**, 127–139.

[17] Brooks HD, Glisson BS, Bekele BN, Johnson FM, Ginsberg LE, El-Naggar A, Culotta KS, Takebe N, Wright J, Tran HT, et al. (2011). Phase 2 study of dasatinib in the treatment of head and neck squamous cell carcinoma. *Cancer* **117**, 2112–2119.

[18] Raju U, Riesterer O, Wang ZQ, Molkentine DP, Molkentine JM, Johnson FM, Glisson B, Milas L, and Ang KK (2012). Dasatinib, a multi-kinase inhibitor increased radiation sensitivity by interfering with nuclear localization of epidermal growth factor receptor and by blocking DNA repair pathways. *Radiother Oncol* **105**, 241–249.

[19] Stegeman H, Kaanders JH, van der Kogel AJ, Iida M, Wheeler DL, Span PN, and Bussink J (2013). Predictive value of hypoxia, proliferation and tyrosine kinase receptors for EGFR-inhibition and radiotherapy sensitivity in head and neck cancer models. *Radiother Oncol* **106**, 383–389.

[20] Bussink J, Kaanders JH, Rijken PF, Martindale CA, and van der Kogel AJ (1998). Multiparameter analysis of vasculature, perfusion and proliferation in human tumour xenografts. *Br J Cancer* **77**, 57–64.

[21] Rijken PF, Bernsen HJ, Peters JP, Hodgkiss RJ, Raleigh JA, and van der Kogel AJ (2000). Spatial relationship between hypoxia and the (perfused) vascular network in a human glioma xenograft: a quantitative multi-parameter analysis. *Int J Radiat Oncol Biol Phys* **48**, 571–582.

[22] Andersson T, Alfredsson L, Kallberg H, Zdravkovic S, and Ahlbom A (2005). Calculating measures of biological interaction. *Eur J Epidemiol* **20**, 575–579.

[23] Lin YC, Wu MH, Wei TT, Chung SH, Chen KF, Cheng AL, and Chen CC (2012). Degradation of epidermal growth factor receptor mediates dasatinib-induced apoptosis in head and neck squamous cell carcinoma cells. *Neoplasia* **14**, 463–475.

[24] Kim MJ, Byun JY, Yun CH, Park IC, Lee KH, and Lee SJ (2008). c-Src-p38 mitogen-activated protein kinase signaling is required for Akt activation in response to ionizing radiation. *Mol Cancer Res* **6**, 1872–1880.

[25] Stegeman H, Kaanders JH, Wheeler DL, van der Kogel AJ, Verheijen MM, Waaijer SJ, Iida M, Grenman R, Span PN, and Bussink J (2012). Activation of AKT by hypoxia: a potential target for hypoxic tumors of the head and neck. *BMC Cancer* **12**, 463.

[26] Rodemann HP, Dittmann K, and Toulany M (2007). Radiation-induced EGFR-signaling and control of DNA-damage repair. *Int J Radiat Biol* **83**, 781–791.

[27] O'Driscoll M and Jeggo PA (2006). The role of double-strand break repair—insights from human genetics. *Nat Rev Genet* **7**, 45–54.

[28] Chen RS, Jhan JY, Su YJ, Lee WT, Cheng CM, Ciou SC, Lin ST, Chuang SM, Ko JC, and Lin YW (2009). Emodin enhances gefitinib-induced cytotoxicity via Rad51 downregulation and ERK1/2 inactivation. *Exp Cell Res* **315**, 2658–2672.

[29] Neal JA, Dang V, Douglas P, Wold MS, Lees-Miller SP, and Meek K (2011). Inhibition of homologous recombination by DNA-dependent protein kinase requires kinase activity, is titratable, and is modulated by autophosphorylation. *Mol Cell Biol* **31**, 1719–1733.

[30] Mahbub Hasan AK, Ijiri T, and Sato K (2012). Involvement of Src in the adaptation of cancer cells under microenvironmental stresses. *J Signal Transduct* **2012**, 483796.

[31] Pham NA, Magalhaes JM, Do T, Schwock J, Dhani N, Cao PJ, Hill RP, and Hedley DW (2009). Activation of Src and Src-associated signaling pathways in relation to hypoxia in human cancer xenograft models. *Int J Cancer* **124**, 280–286.